The Characterisation of Human Body Influence on Indoor 3.5 GHz Path Loss Measurement

Zhihua Lai*†, Nik Bessis*, Guillaume de la Roche*, Pierre Kuonen†, Jie Zhang* and Gordon Clapworthy*

*Institute for Research in Applicable Computing
University of Bedfordshire
Luton LU1 3JU - UK

†GRID and Ubiquitous Computing Group.
University of Applied Sciences of Fribourg
UCH-1705 Fribourg - Switzerland

***Abstract*—This paper investigates the influence of the human body on indoor measurements of radio wave path loss at 3.5 GHz and proposes a solution to improve the accuracy of measurement. The presence of the human body causes measurement errors to radio wave field strength, which is of concern for analysis. The reduction of errors due to measurement process enhances the accuracy of measurement data that is used to validate propagation models. Also, the characterisation of signal strengths at nearby-locations will be presented, which may be used as a proof to develop new propagation models that take advantage of fast calculation based on the observation of relations between geographically-related signal levels. This is also used to analyse the human body influence depending on the locations.**

Index Terms: ***indoor 3.5 GHz measurement, human body influence, radio wave signal strength, spectrum analyser, vector signal generator, propagation modelling***

I. Introduction

The development of an accurate large-scale radio wave propagation model e.g. [1][2] requires validation via measurements. Usually a few locations are selected and signal strengths are recorded. To avoid random effects such as moving crowds or vehicles, several samples have to be taken so to obtain an average signal strength value [3]. Human bodies have a great impact on the signal strength, especially in the case of indoors, where multipath effects are dominant. Indoor high frequency radio wave (e.g. 3.5 GHz) has higher attenuation than a lower frequency. The radio waves at such frequency cannot easily travel behind obstacles [4]. The investigation of the influence of the human body on the high-frequency radio wave propagation is important since this can be used to improve the accuracy of the measurement campaign, which is important when validating indoor propagation models. For example, in [5], the measurement campaign introduced in this paper is used to validate a ray-based indoor model.

The human body has an influence on radio wave measurements. For example, in [6] measurements show that the effect of human body causes fading depths of up to 15 dB. In [7] a conducting cylinder is used to approximate the body presence in the indoor propagation channel. To the best of the authors' knowledge, the influence of the human body on indoor 3.5 GHz path loss measurements has not been previously investigated. The study on this topic is important because 3.5 GHz is the WIMAX (Worldwide Interoperability for Microwave Access) frequency band in Europe. This paper contributes to studying the effects on measurement due to the presence of the human body at this frequency and proposes a solution to reduce the impact of the human body influence.

This paper is organised as follows. First the scenario for indoor measurements is described and the measurement techniques/process are detailed. The analysis of human body influence on the measurements will be analysed and presented. Then, the observations and analysis between geographically-related signal strengths will be presented, which is used to analyse the human body influence depending on its locations. Finally some future work is described which concludes the paper.

II. Measurement Campaign

A measurement campaign has been set up to evaluate indoor propagation models (cf. [5]). This scenario is displayed in Figure 1. It has three rooms and 255 polygons (more than 1,000 vertices) all together. The dimension for this scenario is 16 X 9 X 4 (m^3). The emitter is a vector signal generator (power 6 dBm) equipped with an omni-directional antenna (gain 2.8 dBi, EIRP Equivalent Isotropically Radiated Power 8.8 dBm). A frequency of 3.5 GHz is chosen, which is the frequency of WIMAX in Europe. The emitting signal is CW (Continuous Wave) and narrowband. The antenna is directly installed so no additional cable loss occurs. The emitter is located on the table (1.35 metre height) in the meeting room and measurement locations (0.98 metre height) are positioned by the grid pattern on the floor. Ground-squares patterns are of the size 0.5 metre X 0.5 metre. Measurement locations are denoted by integer coordinates that correspond to the grid positions.

A. Measurement Procedure

To avoid as much noise disruption as possible, a measurement campaign is conducted when there is only one person in the room. A spectrum analyser is used to record the signal strength of radio waves emitted from the vector signal generator. Around 200 points (Figure 2) are positioned by ground floor pattern and distributed in the office. Measurement for these points are split and accomplished during approximately 4 days. These locations are numbered so that the movement and the locations of the spectrum analyser can be indicated without the use of Global Positioning System (GPS).

978-1-4244-6406-7/10/$26.00 ©2010 IEEE

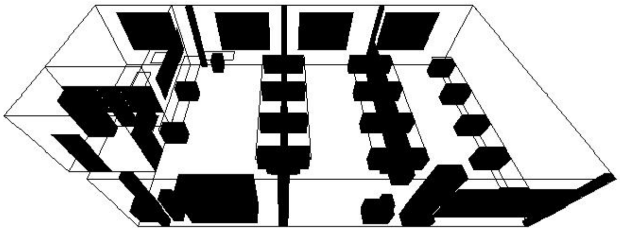

Fig. 1. 3-D view of office

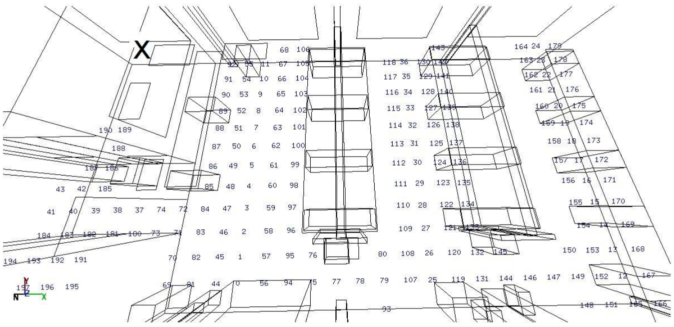

Fig. 2. Measurement locations; 'X' corresponds to antenna position

The spectrum analyser continuously records the radio wave spectrum within a predefined span width. Usually, a larger span width will cause longer scanning time and vice versa. For example, during measurement, if the span width is set to 10 KHz, the time interval between measurement snapshots is around 2 to 3 seconds and if the span width is set to 100 KHz, the corresponding time interval is increased to 12 to 15 seconds.

Several measurement snapshots are required in order to improve the measurement accuracy by reducing the temporary effects such as moving vehicles in the street. The use of GPS [8] repeaters in EU/UK to enhance the reception signal strength indoor is prohibited in order to avoid interference to other GPS users. Therefore, the spectrum analyser may not work with a GPS antenna in indoor measurement process because of the low level of signal strength and/or multipath phenomenons. For outdoor measurements, the GPS can be used to keep positioning information while the spectrum analyser is recording the signal level. In this special case where GPS is not available indoor, a special routine has to be produced to distinguish the files logged by the spectrum analyser and their corresponding positions. The timing intervals between snapshots of measurements are not constant even if a fixed frequency bandwidth is set. This sometimes vary from 1 second to a few seconds, which causes trouble if the time interval is used as a factor to separate measurement logged files. Therefore, this can be solved manually by recording the time periods (start and end), and their corresponding locations. This information can be post-processed (e.g. by a batch script) to extract detailed signal levels from the logged files. The locations are denoted by the grid offsets on the floor. The spectrum analyser is placed one by one on the centres of these grids along the route. The spectrum analyser supports signaling mode, in which it can be set to record or stop automatically by signals captured, which can be used to reduce the influence of the human body. In spite of this, the signaling mode is disabled so the influence of the human body can be investigated.

The procedure is as follows. First record the position of the spectrum analyser, then manually trigger the record button. Quickly move away from the device while it is starting to continually recording the spectrums. Wait approximately 2 minutes before the device records dozens of snapshots and move back to stop the device from recording. The start time of the recording and its corresponding ending time should be recorded onto a worksheet for post-processing at the next stage.

The files logged by the spectrum analyser consist of measurement parameters and most importantly the detailed scan of the frequency spectrums. The signal level (in dBm) for that particular snapshot can be obtained by extracting all these spectrum values. The power p_i (i denotes the index number of measurement points) can thus be calculated as:

$$p_i = \max P_j, j \in [0..N-1]$$

where

P_j denotes the corresponding power level at that particular frequency spectrum.

N denotes the total number of recorded frequency spectrums, usually associated with bandwidth.

Therefore, the values of p_i for the measurement index i can be collected.

Each location requires several measurement snapshots. To avoid the interference of human bodies when manually triggering the spectrum analyser, the measurement data of the first few and last few snapshots are removed. This will be detailed in the next section. The other measurement snapshots are averaged. Spatial filtering [3] is applied in order to remove the fading effects. This is computed by averaging the signal power level (in mW) of one location with its neighbours (the surrounding measurement locations). The distance between neighbours is 0.5 metres, which is approximately 5.8 the wavelength. Figure 3 displays both the filter and unfiltered measurement data. It is observed that, the filtered measurement curve fluctuates less than the unfiltered one (reflecting instant power levels), which is necessary if path loss comparison with the propagation models is of interests.

III. Analysis of the Data

The human body has impacts on measurements if the people stay around the device when the spectrum analyser is recording. For example, measurement point of index 60 consist of 51 snapshots, and is displayed in Figure 4. From the figure, it can seen that the begin and the end measured signal levels are greatly affected by the author (1.75m tall and 65 kg mass, adult male, aged 24, wearing a coat that

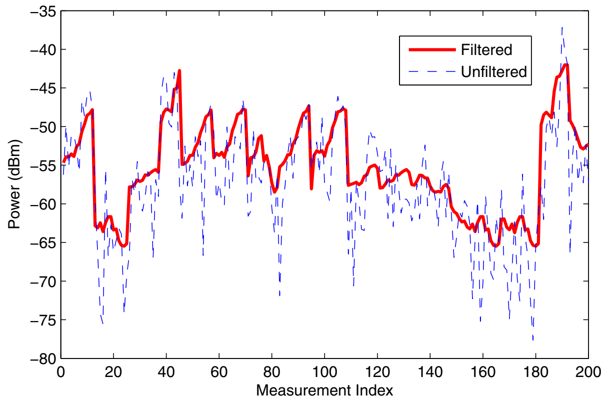

Fig. 3. Spatial filtering applied to remove fading effects

is made of damask) and the values are fluctuating rapidly, which has a 2 to 5 dB difference while the other measured signal levels are within 2 dB difference. Index 1 corresponds to the time 17:03:20 when the author triggers the spectrum analyser and starts to walk away. The presence of the human body can be ignored at index 4 (time 17:03:31) because the author is far away from the spectrum analyser. At index 46 (time 17:05:40), the author quickly walks back to the spectrum analyser and finally at index 51 (17:05:53) the device is turned off. The estimated speed is 3 metres per second. Apparently, the measured values while affected by the human body should be filtered out from measurement data. However, the number of affected measurement snapshots is not easily known and varies from measurement to measurement. This is due to unpredicted time intervals that manually trigger the start/stop button on the spectrum analyser.

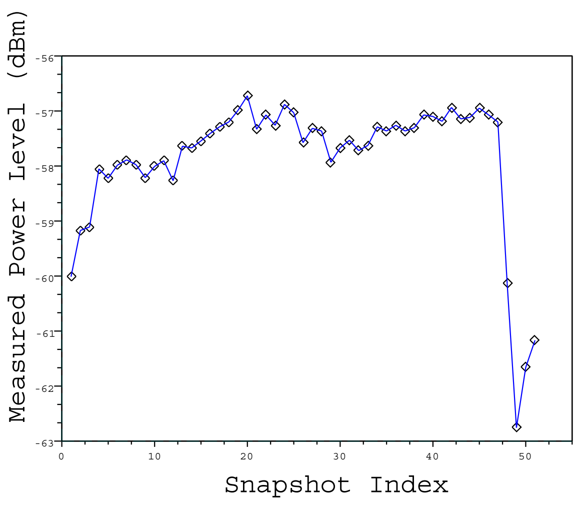

Fig. 4. Snapshots of measurement index 60

To obtain a relatively-accurate measurement profile, Algorithm 1 can be applied, which has the complexity of $O(n)$. It is used to remove severely-affected snapshots at the beginning and the end of the measurement. x represents the starting index position of the measurement snapshots. d is the offset, which can be 1 or -1, denoting the forward or backward scan. The algorithm scans snapshots and removes them if they are likely to be influenced by the human bodies. r ($r \geq 1$) is the minimum number of points that are kept from filtering. The values are checked by computing the difference between the overall mean $\overline{u}$. Δ is used to control the degree of tolerant difference. It takes the array of measurement snapshots $p_i[]$ for index i and the number is denoted as N_p. This procedure filters measurement data and returns the number of abandoned measurement snapshots. Because the measurement errors due to the human body influence are likely to occur at the beginning and the end of measurement snapshots (while the author stands around the spectrum analyser), two filters via this algorithm should be conducted. Filters with $x = 0$, $d = 1$ and $x = N_p - 1$, $d = -1$ denote two scanning forward from the start and backward from the end, respectively. This algorithm is recommended when there are many measurement snapshots ($r \geq 20$) because it may prune out valid snapshots when there are only a few points. It is recommended that, if there are many points, a 'moving average' techniques [9] (averaging measurement data every few points) can be applied to reduce the noise effects, which helps improve the accuracy

Algorithm 1 Filter([in]x, [in]d, [in, out]$p_i[]$, [in, out]N_p, [in]Δ, [in]r)

if $N_p > r$ **then**
  $\overline{u} \leftarrow \frac{\sum_{j=0}^{N_p-1} p_i[j]}{N_p}$
  $j \leftarrow 0$
  $k \leftarrow x$
  while true **do**
    $v \leftarrow p_i[k]$
    if $|\overline{u} - v| \geq \Delta$ **then**
      if $N_p - j > r$ **then**
        $p_i[] \leftarrow p_i[] - v$
        $j \leftarrow j + 1$
      else
        break
      end if
    else
      break
    end if
    $k \leftarrow k + d$
    if ($k < 0$) or ($k > N_p - 1$) **then**
      break
    end if
  end while
  $N_p \leftarrow N_p - j$
  return j
end if
return 0

of this algorithm. For example, for location index 60, 7 points (3 at the beginning and 4 at the end) are filtered ($\Delta = 1$) as the resulting measurement profile is displayed in Figure 5.

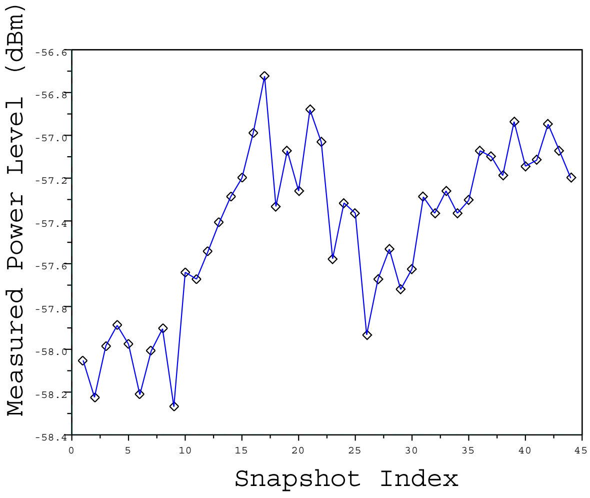

Fig. 5. Filtered snapshots of measurement index 60

By increasing Δ, fewer points are removed and vice versa. The relationship between Δ and the number of eliminated points can be found in Figure 6.

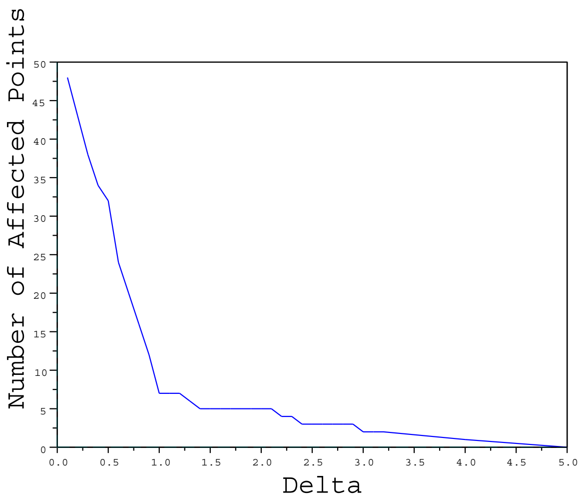

Fig. 6. Δ vs. the number of eliminated points

The final path loss for the measurement index i can be obtained by calculation of Root-Mean-Square (RMS) for the rest of the measurement snapshots i.e.

$$Q_i = \sqrt{\frac{\sum_{j=0}^{N_f-1}(F_i[j]^2)}{N_p - N_f}}$$

where
Q_i is the power level in dBm for measurement index i.
N_f is the number of filtered snapshots.
$F_i[]$ is the unfiltered snapshots array.
N_p is the number of total snapshots.
The path loss for measurement index i can thus be formulated as

$$L_i = P_t - Q_i$$

where
L_i is the path loss (in dB) for measurement index i.
P_t is the emitter power level in dBm.
Without filtering, the calculated path losses have on average approximately 3 to 6 dB difference with the filtered results. In the worst cases, the difference for some locations can reach up to 15 dB. The average number of eliminated measurement snapshots for these 200 points is 9.5. The final measurement path loss profile for these 200 points can be found in Figure 7 (Average 63.45 dB). It is observed that if the human body stays longer at the device, more snapshots will be affected and vice versa.

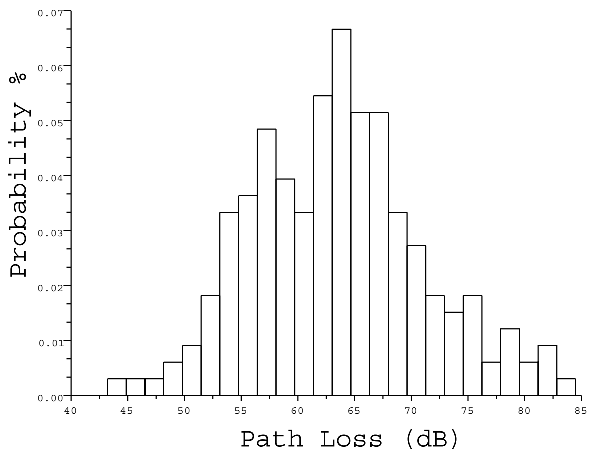

Fig. 7. Histogram of measured path loss

IV. Geographically-Related Human Body Influence

It is of great significance to see the correlations between the human body influence at geographically-related locations. Signal strengths at geographically-related locations are analysed first and the human influence can be investigated. This may be used as an important observation to accelerate propagation models. In this measurement campaign, measurement locations are numbered, which is used to mark the order of measurement. The locations of these points (C_i, i refers to the measurement index) can be denoted by two integer coordinates $[x], [y]$ that represent the offsets of the grids on floor from a reference grid (e.g. lower-left).

Two measurement locations are considered as neighbours if their corresponding coordinates C_i and C_j satisfy

$$|C_i[x] - C_j[x]| \leq 1$$

or

$$|C_i[y] - C_j[y]| \leq 1$$

These neighbour measurement locations are placed next to each other and have a distance of one square (0.5 metre) between them if $C_i[x] = C_j[x]$ or $C_i[y] = C_j[y]$. The distance will be increased to 0.707 metre if two measurement locations are diagonal. Therefore, a measurement location will have a maximum number of 8 neighbours. To investigate the similarity between these neighbour measurements, the function $\mu(i)$ is defined as

$$\mu = \sqrt{\frac{\sum_{k=0}^{N_n-1}((L_i - L_{N(i,k)})^2)}{N_n}}$$

where
i is the measurement index.
L_i is the measured path loss for index i.
N_n is the number of neighbours for measurement location i ($N_n > 0$).
$N(i,k)$ returns the index of the number k neighbour of measurement location i.

$\mu(i)$ computes the RMSE (Root Mean Square Error) between measurement index i and its corresponding neighbours. The resulting μ for all neighbours can be investigated by plotting their histograms of using neighbours of distances 0.5 metres or 0.707 metres, and all neighbours (Figure 8, 9 and 10) respectively. The average score value μ is around 6, which indicates the neighbour signal strengths usually vary within 6 dB in this special scenario. It is also observed that with a slight increase of distance (from 0.5 to 0.707 metre), the average μ is increased from 5.79 to 6.05, which indicates that if the distance between points is increased, so is the difference of power level between them. It is also observed that there is no strong correlation between μ and the distance to emitter, which indicates that μ is independent of distance. The measurement errors due to human body exist no matter how far the measurement location is from the emitter.

The correlation between μ and the number of snapshots removed by Algorithm 1 is displayed in Figure 11. The "+" sign shows the number of removed snapshots and the red line displays the μ. The plot indicates a strong correlation between these two factors for the major measurement locations. The correlation can be calculated [9] as:

$$\mathrm{C}(N,\, M) = \frac{\sum i = 1^n((N_i - \overline{N})(M_i - \overline{M}))}{\sqrt{\sum i = 1^n(N_i - \overline{N})^2 \sum i = 1^n(M_i - \overline{M})^2}}$$

where
$N,\, M$ are two series of data.

In this case, the correlation is 86.32%. From Figure 11, it indicates that the human influence may be strongly correlated in some locations i.e. the locations can be identified in clusters of small regions where the human influence score (μ) are relevant: a larger μ causes more snapshots to be removed, and vice versa. This can be explained by the situation that, in some locations such as corners or windows, when the author turns on the spectrum analyser, he blocks the dominant rays from emitter and therefore the human body influence to the final signal strength is significant.

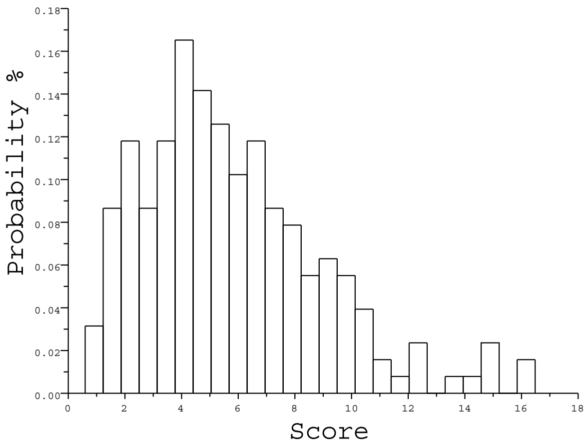

Fig. 8. Histogram of μ for neighbours (0.5 metre) average = 5.79

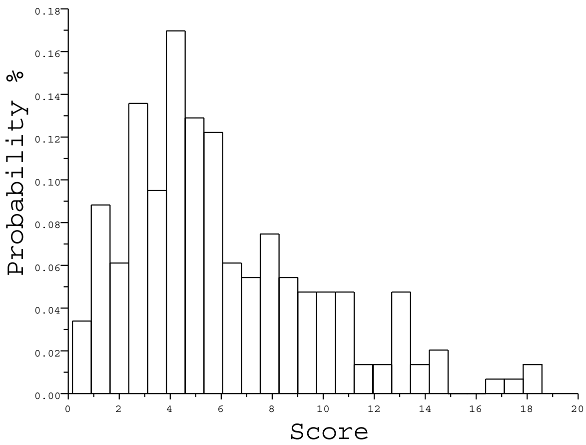

Fig. 9. Histogram of μ for neighbours (0.707 metre) average = 6.05

V. Conclusion

This paper describes a measurement campaign conducted in an office. Data collected is analysed and the influence of the human body on measurements is investigated. The procedure to reduce the effects and improve the measurement accuracy is proposed. The correlations of the measurements that are geographically-related are investigated and the results show that the degree of average variance of measured signal strength

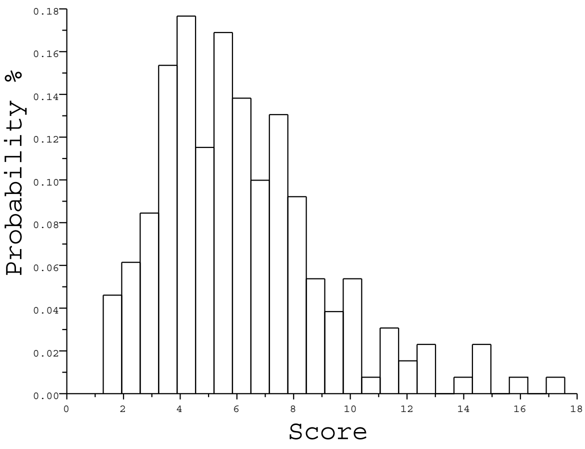

Fig. 10. Histogram of μ for all neighbours

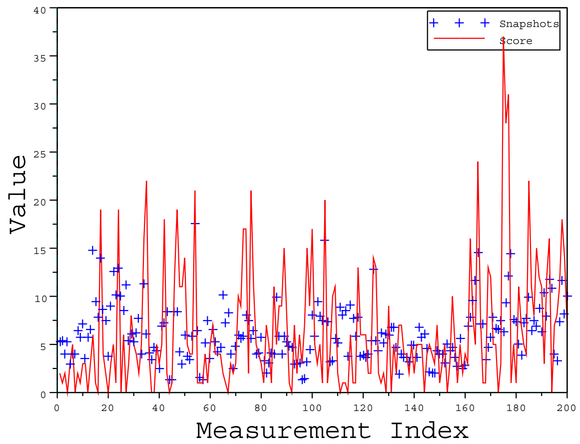

Fig. 11. Correlation between μ and points removed

increases when the distance between two geographically-related locations is increased. The correlation between human body influence function and the number of snapshots removed by the proposed algorithm is investigated, which may indicate there is a strong correlation between the human body influence and locations, at least from this measurement campaign. Future work involves conducting more measurements at different frequencies and analysing the effect of the human body at these different frequencies. Furthermore, the investigation on the correlation between the human body influence and different scenarios may be considered.

ACKNOWLEDGEMENTS

This work is supported by the EU-FP7 iPLAN and FP6 GAWIND under grant number MTKD-CT-2006-042783 ("Marie Curie Fellowship for Transfer of Knowledge"). The authors would also like to thank Malcom Foster for his valuable corrections of this paper.

REFERENCES

[1] Z. Lai, N. Bessis, G. De La Roche, H. Song, J. Zhang, and G. Clapworthy. An intelligent ray launching for urban propagation prediction. In *The Third European Conference On Antennas and Propagation*, pages 2867–2871, Berlin, Germany, March 2009.

[2] A. Valcarce, G. De La Roche, and J. Zhang. On the use of a lower frequency in finite difference simulations for urban radio coverage. In *IEEE Vehicular Technology Conference*, pages 270–274, Marina Bay, Singapore, May 2008.

[3] A. Valcarce, G. De La Roche, A. Juttner, D. Lopez, and J. Zhang. Applying FDTD to the coverage prediction of WiMAX femtocells. *EURASIP Journal of Wireless Communications and Networking*, 2009.

[4] M. Khrouf, M. Ayadi, S. Ben Romdhane, N. Saghrouni, S. Tabbane, and Z. Belhadj. Indoor prediction of propagation using dominant path: Study and calibration. In *the 12th International Conference on Electronics, circuits and Systems, ICECS 05*, December 2005.

[5] Z. Lai, N. Bessis, G. De La Roche, P. Kuonen, J. Zhang, and G. Clapworthy. On the use of an intelligent ray launching for indoor scenarios. In *The Fourth European Conference On Antennas and Propagation*, Barcelona, Spain, April 2010.

[6] K. Ali. Human body shadowing variability in short-range indoor radio links at 3-11 GHz band. *International journal of electronics*, 96, 2009.

[7] M. Ghaddar, L. Talbi, T.A. Denidni, and A. Sebak. A conducting cylinder for modeling human body presence in indoor propagation channel. *IEEE Transactions on Antennas and Propagation*, 55, 2007.

[8] B.W. Parkinson. *Global Positioning System: Theory and Applications*. American Institute of Aeronautics and Astronautics, 1996.

[9] E. Weisstein. Making mathworld. *The Mathematica Journal*, 10, 2005.